Journal of Biotechnology 399 (2025) 9–18

Contents lists available at ScienceDirect

Journal of Biotechnology

journal homepage: www.elsevier.com/locate/jbiotec

Interferon inhibitors increase rAAV production in HEK293 cells

Yongdan Wang [a,*], Qiang Fu [b], Sha Sha [a,*], Seongkyu Yoon [a,*]

[a] Department of Chemical Engineering, University of Massachusetts Lowell, Lowell, MA 01854, United States
[b] Department of Biomedical Engineering and Biotechnology, University of Massachusetts Lowell, Lowell, MA 01854, United States

ARTICLE INFO

Keywords:
gene therapy
rAAV production
HEK293 cells
innate immune response
unfolded protein response (UPR)
interferon (IFN) inhibitors

ABSTRACT

Recombinant adeno-associated viruses (rAAVs) comprise a promising viral vector for therapeutic gene delivery to treat disease. However, the current manufacturing capability of rAAVs must be improved to meet commercial demand. Previously published omics studies indicate that rAAV production through transient transfection triggers antiviral responses and endoplasmic reticulum stress responses in the host cell. Both responses negatively regulate viral production. We demonstrate that the modulation of the antiviral immune response (by blocking interferon signaling pathways) can effectively lower the production of interferon and enhance viral genome production. The use of interferon inhibitors before transfection can significantly increase rAAV production in HEK293 cells, with up to a 2-fold increase in productivity and up to a 6-fold increase in specific productivity. Compared to the untreated groups, the addition of these small molecules generally reduced viable cell density but increased vector productivity. The positive candidates were BX795 (a TBK inhibitor), TPCA-1 (an IKK2 inhibitor), Cyt387 (a JAK1 inhibitor), and ruxolitinib (another JAK1 inhibitor). These candidates were identified using deep well screening, and reproducible titer improvement was achieved in a 30 mL shake flask scale. Additionally, genome titer improvement is feasible and scalable in two different media, but the extent of improvement may vary.

1. Introduction

rAAVs serve as a commonly utilized viral vector in gene therapy due to their safety, persistence, and their ability to infect a wide range of cells (both dividing and non-dividing) efficiently in various tissues (Fu et al., 2023). Current triple transient transfection platforms for AAV production are still inefficient, and they require considerable improvement because the use of rAAV–based gene therapy is growing (Fu et al., 2023). Transfection parameter optimization through design of experiments (DOE) has been widely conducted to improve the process and to enhance rAAV productivity (Fu et al.; Zhao et al., 2020). Still, these improvements may be restricted to specific cell lines or to specific media. Thus it is critical to gain insights into the molecular mechanisms that support rAAV production in host cell lines such as HEK293.

A systematic analysis of host cells can help identify strategies to modulate cellular pathways (e.g., small-molecule additives, cell-line engineering strategies) to optimize AAV manufacturing processes (Wang et al., 2024). Previous omics studies reveal that transfection and rAAV production trigger a strong defense response from the host cell, including both inflammatory responses and antiviral responses (Chung et al., 2023; Lu et al., 2024; Wang et al., 2023; Warga et al., 2023). Upregulated IFN-stimulated genes have been shown to substantially

Abbreviation: AAV, adeno-associated virus; AZD1480, 5-chloro-N2-[1S-1–5-fluoro-2-pyrimidinylethyl]-N4-5-methyl-1H-pyrazol-3-yl-2,4-pyrimidine-2,4-diamine; *BCl2,*, B-cell leukemia / lymphoma 2; BX 795, N-[3-[[5-iodo-4-[[3-[2-thienylcarbonylamino]propyl]amino]-2-pyrimidinyl]amino]phenyl]-1-pyrrolidinecarboxamide; CYT387, N-cyanomethyl-4-[2-[[4–4-morpholinylphenyl]amino]-4-pyrimidinyl]-benzamide; ER, endoplasmic reticulum; *GADD34,*, growth arrest and DNA damage inducible protein 34; HEK, human embryonic kidney; HSPA, heat shock protein family A; IFIT, interferon-induced protein with tetratricopeptide repeats; IFN, interferon; IFNAR, interferon alpha receptor; ISG, interferon stimulated genes; IKK2, IkappaB kinase; IRF, interferon regulatory factor; JAK1, Janus kinase 1; ML346, e-5–3-(4-methoxyphenylallylidene)pyrimidine-2,4,61h,3h,5h-trione; NF-kB, nuclear factor kappa B; *OAS1,*, oligoadenylate synthetase 1; PDK1, 3-phosphoinositide-dependent kinase 1; PKR, protein kinase R; RSAD2, radical S-adenosyl methionine domain containing 2; STAT, signal transducer and activator of transcription 2; TBK1, TANK binding kinase 1; TPCA-1, 2-[aminocarbonylamino]-5–4-fluorophenyl-3-thiophenecarboxamide; TRC051384, *n*-[2–4-morpholinylethyl]-*n*′-[4-[3-[6–4-morpholinyl-2-pyridinyl]-1-oxo-2-propen-1-yl]phenyl]urea; TYK2, tyrosine kinase 2; UPR, unfolded protein response; VCD, viable cell density; *XBP1,*, X-box binding protein 1.

* Correspondence to: 1 University Ave, Lowell, MA 01854, United States.
E-mail addresses: xiami1117@gmail.com (S. Sha), seongkyu_yoon@uml.edu (S. Yoon).

https://doi.org/10.1016/j.jbiotec.2025.01.009
Received 12 May 2024; Received in revised form 17 December 2024; Accepted 13 January 2025
Available online 15 January 2025

impede viral genome replication and production. These genes include *RSASD2* (Dumbrepatil et al., 2019; Ebrahimi et al., 2020; Honarmand Ebrahimi et al., 2020), *OAS* family genes (Drappier and Michiels, 2015), and *IFIT* family genes (Zhou et al., 2013).

Furthermore, a proteomic study of HEK293 cells during the production of adeno-associated virus type 5 (AAV5) demonstrates that numerous differentially expressed proteins participate in cell proliferation, defense responses, and metabolic processes (Strasser et al., 2021). Thus, the control of antiviral responses triggered by host–virus interactions (e.g., restricting IFN production and ISG expression) are likely beneficial for viral production. In addition, the overexpression of protein chaperone *HSPA6* (Hsp70, a heat shock protein) was observed in the *viral-producing* cultures from an earlier transcriptomic study (Wang et al., 2023). This heat shock protein helps modulate the unfolded protein response and relieves ER stress. The modulation of ER protein processing through the addition of chemical chaperones likely enhances cell productivity.

Small molecules have been extensively utilized in mammalian cells to improve vector production (Scarrott et al., 2023) and therapeutic protein production (Allen et al., 2008; Chang et al., 2020; Meyer et al., 2017; Yang et al., 2014). IFN-signaling protein inhibitors (e.g., BX795 (a TBK1 inhibitor), TPCA-1 (an IKK2 inhibitor), ruxolitinib (a JAK1 inhibitor)) have been utilized to block the induction of IFN and to restrict the expression of ISGs; and these inhibitors successfully attenuated the innate immune responses and enhanced the replication of respiratory syncytial virus and the influenza virus (Stewart et al., 2014). Moreover, a significant 3-fold increase in rAAV8 genome titer has been achieved through the combined addition of nocodazole (a mitosis inhibitor) and M344 (a histone deacetylase inhibitor) (Scarrott et al., 2023).

In addition, chemical chaperones (e.g., trehalose, proline, glycerol) have been reported to increase recombinant protein productivity and to decrease protein aggregation (Hwang, Jeon, Cho, Lee, and Yoon, 2011; Onitsuka et al., 2014). The effective impact of these small-molecule additives on viral titer, the simple addition process, and a successful proof-of-concept study (Stewart et al., 2014) make IFN–inhibitor supplementation a novel and attractive control strategy to assess during rAAV production. Due to the cytotoxicity of small-molecule additives (Stewart et al., 2014) and difference in the cell lines, the appropriate dose ranges for HEK293 cells needs to be determined.

In this study, we conducted a high-throughput deep well plate screening of chemical additives that target innate immune responses and ER stress for rAAV production based on the pathways identified from an earlier transcriptomics study (Wang et al., 2023). We evaluated a series of doses during cell growth and determined the appropriate dosing for each additive during rAAV production in the deep well. We chose the most promising candidates that demonstrated positive effects on productivity, and we confirmed their effects on viral vector yields in the shake flasks. Based on the mechanism of action (MOA), the biological function of these additives was validated based on IFN gene expression changes before and after supplementation. Furthermore, we demonstrate that, with an optimized dose, the inhibition of IFN signaling pathways effectively improve vector productivity by up to 2-fold and can increase vector productivity by up to 6-fold. Also, the behavior of specific additives varies in different cell culture media, at different scales, and based on other factors.

2. Materials and methods

2.1. Cell culture and AAV vector production in suspended HEK293 cells

An HEK293 cell line was purchased from ATCC ([HEK-293] CRL-1573, ATCC) and adapted to two different media: AMBIC 1.0 HEK-293 in-house medium supplemented with 4 mM GlutaMax™ (Thermofisher, United States) and BalanCD HEK-293 medium (Irvine, United States) with 4 mM glutamine (Thermofisher, United States) added. Cells were cultured in shake flasks (5 % CO_2, 37 °C, shaking at 125 rpm). For the initial small-scale screening, cultures were transfected in the 24-well plates (3 mL culture volume per well, 5 % CO_2, shaking at 300 rpm) using a clamping system (EnzyScreen BV, Netherlands) (Duetz et al., 2000). For the shake flask confirmation experiments, the transfection process utilized 30 mL of cell culture in a 125 mL shake flask. Daily cell density and cell viability measurements were performed using a Cedex® HiRes Analyzer (Roche Life Science, United States). rAAV viral vectors were produced using the triple transient transfection method previously described (Wang et al., 2023).

2.2. Chemical additive screening in deep well plates

Inhibitors of the IFN responses (i.e., BX795, TPCA-1, Cyt387, AZD1480, ruxolitinib, tofacitinib, and deucravacitinib) and the activators of *HSP70* (ML346, TRC051384) were diluted as 10 mM stocks in dimethyl sulfoxide (Sigma Aldrich, United States) (DMSO, 100 % v/v) and used as the indicated concentrations. The chemical additives used for screening were all purchased from MedChemExpress. Before screening, we examined the impact of small-molecule additives on cell growth and viability (data not shown). The concentration range for each chemical additive was based on the available literature as well as vendor recommendations (see Table 1). *Low*, *middle* (mid), and *high* concentrations were further defined after the initial screening (see Table 3). Inhibitors of the IFN responses were added 4 h before transfection to ensure they effectively performed their intended biological functions on the cell culture. The time course addition of the *HSP70* activator was also investigated 4 h before transfection, 24 h post transfection (HPT), and 48 HPT. Cells were initially grown to the mid-exponential phase in the shake flasks, then adjusted to the target cell density, and then aliquoted to the 24 deep well plates (Enzyscreen BV, Netherlands). To rule out the impact of DMSO on cell growth and viral titer, two control conditions were used: one control without DMSO, and one control with the addition of a maximized concentration of DMSO used for supplements. We prepared the transfection reaction in one tube, and then aliquoted this evenly into the deep well plates. Cell cultures were harvested 72 HPT for genome titer measurement using qPCR.

2.3. rAAV viral vector genome titer

The crude harvest samples were treated, and the quantification of viral titer could be achieved along with six reference standards, as previously described (Wang et al., 2023). The primer and probe sequences used for the genome titer were:

Forward: 5′- GAA CCG CAT CGA GCT GAA −3′

Reverse: 5′- TGC TTG TCG GCC ATG ATA TAG −3′

Probe: /56-FAM/ATC GAC TTC /ZEN/AAG GAG GAC GGC AAC /3IABkFQ/

The specific productivity can be calculated as

$$IVCD = \frac{(VCD_2 + VCD_1) \times (t_2 - t_1)}{2} \quad (1)$$

$$Q_p = \frac{Titer_2 - Titer_1}{IVCD} \quad (2)$$

Note that *VCD* refers to viable cell density expressed as millions of cells per mL; VCD_1 and VCD_2 refer to the viable cell densities collected at time points t_1 and t_2, respectively; *IVCD* represents the integral viable cell concentration expressed in cell·h/mL; and Q_p stands for specific productivity expressed in viral genome/cell·h. The final titer and cell density at harvest ($Titer_2$) and the seeding density ($Titer_1$) were used to calculate Q_p.

2.4. RNA isolation and cDNA reverse transcription

For shake flask confirmation experiments, samples were collected daily after transfection to verify gene expression. Approximately

Table 1
Tested medium supplements, their functions, and the tested dose ranges used.

Compound #	Supplement categories	Functions	Small molecule names	Suggested dose ranges	Catalog No.
S1	interferon signaling pathways	TBK inhibitor	BX795	0–4 μM	HY−10514
S2		IKK2 inhibitor	TPCA−1	0–4 μM	HY−10074
S3		JAK1 inhibitor	Cyt387	0–4 μM	HY−10961
S4			AZD1480	0–4 μM	HY−10193
S5			ruxolitinib	0–4 μM	HY−50856
S6			tofacitinib	0–4 μM	HY−40354
S7		TYK inhibitor	deucravacitinib	0–10 μM	HY−117287
S8	unfolded protein response	HSP70 activator	ML346	0–10 μM	HY−18669
S9			TRC051384	0–10 μM	HY−101712
DMSO					D8418-mL

2×10^6 cells were centrifuged (at 1250 rpm for 5 min) from the cell suspension. The cell pellets were washed twice with iced PBS and then stored at −80 °C. Total RNA was extracted using the RNeasy Mini Kit (QIAGEN, United States) with DNase digestion (QIAGEN, United States) following the manufacturer's instructions. We performed a second DNase I digestion (DNase I, Amplification Grade, Invitrogen) to eliminate any DNA before PCR amplification according to the instructions. Then, first-strand cDNA was synthesized from the total RNA using a SuperScript III First-Strand Synthesis System purchased from Invitrogen according to the instructions. Random hexamers were used as primers for cDNA synthesis reactions. RNase H digestion was then conducted to remove the RNA template after first-strand synthesis.

2.5. Gene expression by RT-PCR

Synthesized cDNA samples were diluted 10 times, amplified, and detected in a qPCR using the universal SYBR Green (Thermo Fisher, United States) protocol. The comparative cycle threshold ($2^{-\Delta\Delta Ct}$) method was employed to assess the changes in relative gene expression levels. The transcript level was standardized using the housekeeping gene *GAPDH*. The relative gene expression for each sample was quantified in technical duplicates.

The primer sequences used for the IFN-β and *GAPDH* expression are:
GAPDH Forward: 5′-CCCACCACACTGAATCTCCC-3′
GAPDH Reverse: 5′-TACATGACAAGGTGCGGCTC-3′
IFN-β Forward: 5′-GGCACAACAGGTAGTAGGCG-3′
IFN-β Reverse: 5′-GTGGAGAAGCACAACAGGAGA-3′

3. Results

3.1. Transcriptomic results and supplement candidates

Our recent transcriptomic results reveal that innate immune responses and host cellular stress responses (e.g., ER stress, apoptosis) are significantly upregulated in *viral-producing* cultures relative to *non-producing* cultures in HEK293 cells over time (Wang et al., 2023). The production of interferons (IFNs) and the initiation of IFN–stimulated genes (ISGs) in the innate immune response pathways of the host cell have been shown to adversely affect viral replication and production (Wang et al., 2023). This suggests that modulation of these innate immune pathways might enhance viral production.

Stewart et al. evaluated a range of small-molecule inhibitors that might target IFN signaling pathways. They successfully demonstrated the ability to block IFN pathways, lower innate immune responses, and enhance the replication of various virus types (Stewart et al., 2014).

Fig. 1 shows the workflow of the medium supplement study. We chose candidates for supplementation based on previous transcriptomic studies, while focusing on the significantly enhanced innate immune responses and ER stress responses observed during rAAV production. Initial high-throughput screenings were conducted in 24-deep well plates. Promising candidates were then evaluated at their respective optimal doses using shake flasks. We assessed the functionality of small-molecule inhibitors by measuring gene expression.

Table 1 shows the types, names, and functions of these small molecules. S1–S7 were selected to inhibit the signaling proteins (e.g., TBK, IKK2, JAK1, TYK) involved in IFN induction pathways. S8 and S9, as activators of molecular chaperones, were chosen to reduce ER stress and unfolded protein responses. Specifically, BX795 (S1) is a TBK inhibitor,

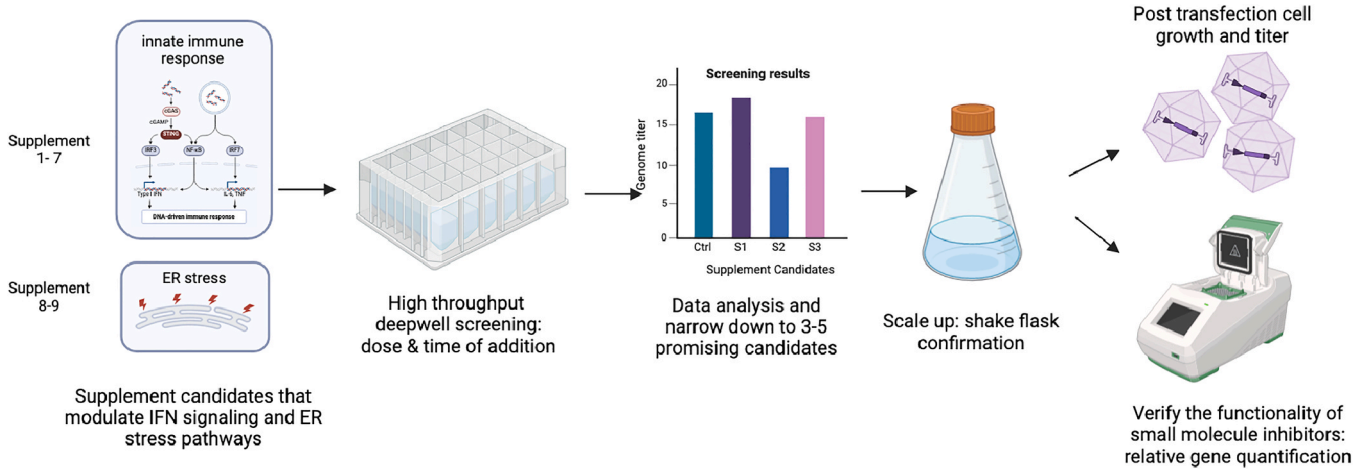

Fig. 1. Workflow of the medium supplement study. Supplement candidates were selected based on prior transcriptomic results; specifically, highly enriched innate immune responses and ER stress responses during rAAV production. High-throughput screenings were initially performed in the 24 deepwell plates. The behavior of promising candidates in their respective optimal doses were further confirmed using a shake flask. Gene expression was measured to evaluate the functionality of small molecule inhibitors. The figure was created using BioRender.

and TPCA-1 (S2) inhibits IKK2. Cyt387, AZD1480, ruxolitinib, and tofacitinib (S3–S6) target JAK1, and deucravacitinib (S7) inhibits TYK. ML346(S8) and TRC051384 (S9) are chaperone (*HSP70*) activators that alleviate unfolded protein responses. Detailed information on these pathways can be found in the previous transcriptomic analysis paper (Wang et al., 2023).

The dose ranges for IFN signaling inhibitors were 0–4 μM, based upon the screening ranges set in the literature (Stewart et al., 2014) because concentrations beyond this range potentially decrease cell viability. These IFN inhibitors were added to the cell culture medium 4 h before transfection to ensure sufficient inhibition activity targeting IFN signaling pathways (Stewart et al., 2014). The dose ranges for chaperone activators were set to 0–12 μM based on the literature or the user manual from MedChemExpress (Calamini et al., 2013; Mohanan et al., 2011). Different addition times were studied for chaperone activators because ER stress is typically triggered during transfection and viral production by the large accumulation of synthesized viral proteins.

3.2. Deep well screening of chemical additives

To identify the general viral vector productivity enhancers in the HEK293 cells, two media were used for this study: commercial BalanCD_HEK293 and in-house AMBIC_HEK293. Table 2 and Supplementary Table 2 show the transfection parameters for viral production in the BalanCD and AMBIC media. Two rounds of high-throughput screening experiments were conducted in biological duplicates in the deep well plates. The impact of these additives on cell viability was evaluated at 0.5 μM, 1 μM, 2 μM, and 4 μM before screening (data not shown), and the maximum doses (resulting in >60 % viability) were selected for Screening 1, which evaluated the potential impact of these chemical additives on post-transfection cell growth and viral productivity. Based on the results of Screening 1, the dose ranges for promising candidates were then adjusted, and these doses were evaluated further in Screening 2.

Fig. 2(a) shows the results of deep well Screening 1 in the BalanCD medium 72 h post transfection (72 HPT). After transfection, S4-S9 cultures exhibited more cell growth than the control, while S1-S3 cultures showed inhibited cell growth (see Supplementary Table 3). In terms of productivity (see Fig. 2(a)), the S1–S3 and S5 cultures exhibited comparable or higher genome titer yield compared to the control group, while other cultures displayed reduced productivity in their respective concentrations. We observed that a considerable quantity of medium had evaporated from one biological replicate of the S2–2 culture in the deep well due to its position on the edge of the deepwell apparatus. This caused an elevated false positive signal and a large error bar for the S2–2 cultures.

We explored the dose ranges of promising candidates based on the results of Screening 1; the *low/mid/high* concentrations were shown in Table 3 for each supplement in Screening 2. These *low/mid/high* dose settings were established to obtain the optimal dose for the candidate supplement, thus achieving a balance between maintaining acceptable cell growth while maximizing productivity after transfection. Supplements were dissolved and prepared in DMSO. *Control* (DMSO) represents the control condition with the maximum volume of DMSO (36 μL, 100 % DMSO, with a 3 mL working volume) used to dilute supplements. Fig. 2(b) shows the results of Screening 2 in the BalanCD medium. Figs. 3 and 4 provide details on viral titer and VCD averages for each supplement with varying concentrations 72 HPT in the BalanCD medium. Supplementary Table 4 shows details for the VCD replicates.

Table 2
Transfection parameters for viral production in BalanCD cell cultures.

Parameters	Unit	Settings
Initial seeding density	10^6 cells/mL	2
PEIpro:DNA mass ratio		1:1
Total DNA per cell	pg/cell	0.75
Plasmid molar ratio (Helper:Repcap:GOI)		1:1:1
Cocktail volume	volume percentage	10 %
Incubation time	min	15

S1-BX795, an inhibitor of the TBK signaling protein, was the most promising supplement in the BalanCD cell culture. With a 0.25–1 μM supplementation, S1-BX795 increased viral titer by 1-fold to 3-fold, but it also significantly decreased VCD in 0.5 μM and 1 μM compared to the control (see Fig. 3(a)). A supplementation of 1 μM S2-TPCA-1 enhanced cell growth performance and increased viral titer by 20 % compared to the control condition, while other concentrations showed either a similar or decreased yield (see Fig. 3(b)). S3-Cyt387 exhibited the best performance with 1 μM. It improved viral production by 2.5-fold along with an increase in VCD (see Fig. 3(c)). Additionally, a 2 μM supplementation of S5-ruxolitinib (an inhibitor of JAK1) increased viral productivity by 2-fold while increasing VCD (see Fig. 3(e)).

On the other hand, S4 (see Fig. 3(d)), S6 (see Fig. 3(f)), S7 (see Fig. 3(g)), and S8–S9 (Figs. 4(a) and 4(b)) demonstrated either a decline or an insignificant increase in viral titer within the specified concentration range. Generally, VCD tended to decrease as the supplement concentration increased. Overall, the inhibition of IFN signaling proteins (including an TBK inhibitor (S1), an IKK2 inhibitor (S2), and JAK1 inhibitors (S3 and S5)) enhanced viral productivity to various extents, and each small molecule compound in the BalanCD medium showed a different optimal supplementation dose.

In addition to our investigation of the impact of dosage levels on viral productivity, we further explored optimal times for the addition of additives related to ER stress (S8 and S9 in Figs. 4(c) and 4(d)). This exploration considered that ER stress is usually triggered during transfection and viral production due to the significant accumulation of synthesized viral proteins. As shown in Fig. 4, S8-ML346 (an *HSP70* activator) achieved a titer improvement of approximately 50 % with 4 μM of supplementation when added 24 h post transfection. Because most viral components are synthesized the first day after transfection, we added small molecules 24 h post transfection to alleviate ER stress and potentially enhance viral vector production. We observed almost no titer change when small molecules were added 48 h after transfection. Several factors could contribute to this observation. First, small molecules need time to function properly in cell cultures. Additionally, AAV production typically requires a 3-day cultivation period, and 48 h post transfection is approaching the later production phase.

We applied the same screening methods to the HEK293 cell cultures in the AMBIC medium to evaluate whether the positive impact of IFN inhibitors on viral vector productivity were applicable across different media. The optimal genome titer of the control group obtained in the AMBIC medium was 3 times lower than the control group in the BalanCD medium. Supplementary Figure 1 shows the result of deep-well Screening 1 in the AMBIC medium. The behavior of individual chemical supplements on post-transfection cell growth and rAAV production in the AMBIC medium differed slightly from the supplements in the BalanCD medium. However, the overall trend in the BalanCD medium appeared to be similar in terms of inhibited cell growth and improved viral productivity.

In terms of VCD, the majority of supplements (in their respective concentration conditions) exhibited comparable cell growth to the control condition on Day 3 post transfection. The addition of S4, S5, and S9 increased genome titer, while the supplementation of all other small molecules in their respective concentrations resulted in reduced or comparable productivity (see Supplementary Table 5). Similarly, in Screening 2 (See Supplementary Table 6), dose ranges in the AMBIC medium were set for each supplement based on the results of Screening 1 and based on partial results from the BalanCD medium screening experiments. Supplementary Table 1 shows the *low/mid/high* concentration levels. Supplementary Figure 1(b) provides detailed information on the viral titer for each concentration on Day 3 post transfection. To be specific, a 1 μM supplementation with S2-TPCA1 and a 0.5 μM

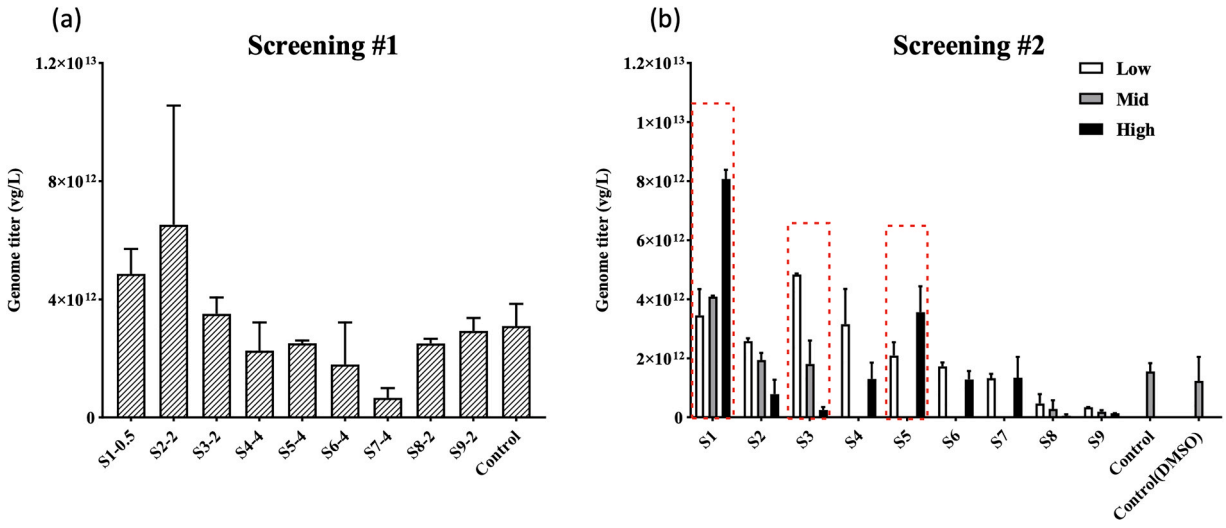

Fig. 2. Deep well screening for AAV2 production in HEK293 cells in BalanCD medium: (a) genome titer in Screening 1 in vg/L 72 h post transfection (HPT), (b) genome titer in Screening 2 in vg/L 72 HPT. The error bar represents the mean and standard deviations for biological duplicates ($n = 2$). The *x* axis shows the supplement number and its selected concentration used in Screening 1. Refer to Table 1 for the *low/mid/high* concentrations of each supplement used in Screening 2. The promising candidates are highlighted in the red boxes.

Table 3
Low/mid/high doses used for BalanCD cell cultures in Screening 2.

	BalanCD		
μM	**low**	**mid**	**high**
S1	0.25	0.5	1
S2	1	2	4
S3	1	2	4
S4	1	NA	2
S5	1	NA	2
S6	1	NA	2
S7	1	NA	2
S8	4	8	12
S9	4	8	12

Note: Among these doses, *mid* doses for S4–S7 were not evaluated due to the relatively narrow gap between the *low* and *high* doses.

supplementation with S3-Cyt387 improved the rAAV titer slightly, while other supplements demonstrated a comparable or reduced rAAV genome titer compared to the control condition in the AMBIC cell cultures.

3.3. Scale-up shake flask confirmation runs

We chose several promising supplements (S1–S3 and S5) based on the results of Screening 2, applied their optimal doses to cultures separately, and further verified productivity improvement in a 30 mL working volume in 125 mL shake flasks. Specifically, for BalanCD cell cultures, 1 μM S1, 1 μM S2, 1 μM S3, and 2 μM S5 were selected for the shake flask confirmation run. For the AMBIC cell cultures, 0.5 μM S1, 1 μM S2, 0.5 μM S3, and 1 μM S5 were selected for the confirmation run. S1, S2, S3, and S5 were added 4 h before transfection. Fig. 5 shows the genome titer and specific productivity for both the supplemented groups and the control in the BalanCD medium. Supplementary Figure 2(a) provides details about supplement behavior in the AMBIC medium.

The IFN inhibitors (S1, S2, S3, and S5) exhibited a positive impact on genome titer compared to the control condition. This trend was consistent with the trend observed in the deep well screening. Cell growth was reduced for all the cultures supplemented with IFN inhibitors. Given their respective optimal doses in different media, IFN inhibitors showed more obvious productivity improvement in the BalanCD medium. Specifically, these improvements were (in vg/L): a 2-fold increase with S1 ($p = 8.43 \times 10^{-3}$), a 20 % increase with S2 ($p = 0.0222$), a 2-fold increase with S3 ($p = 3.77 \times 10^{-4}$), and a 1.5-fold increase with S5 ($p = 2.60 \times 10^{-5}$) (see Fig. 5(a)). Supplementary Table 7 provides more details about VCD and genome titer in BalanCD medium in shake flask run.

Fig. 5(b) shows that S1 resulted in a 6-fold increase in specific productivity (Q_p) in vg/cell ($p = 6.81 \times 10^{-3}$), while up to 2-fold increase in Q_p was observed for S2 ($p = 0.039$), S3 ($p = 7.57 \times 10^{-3}$), and S5 ($p = 5.883 \times 10^{-3}$). However, when these IFN inhibitors are added in their respective optimal doses in the AMBIC medium, they demonstrate less productivity improvement, up to 30–50 % titer improvement (see Supplementary Figure 2).

3.4. Verification of gene expression levels

Theoretically, TBK1 inhibitor S1 (BX795), IKK2 inhibitor S2 (TPCA-1), and JAK1 inhibitors S3 (Cyt387) and S5 (ruxolitinib) all target the IFN signaling pathways. Stewart et al. selected the IFN-β gene expression to evaluate the IFN signaling pathways (Stewart et al., 2014) because IFN was produced when the host cell recognizes viral components, and this further triggers downstream JAK–STAT pathways and ISG transcription. The pivotal role of IFN thus can be utilized to assess signaling transduction status (Stewart et al., 2014). To assess IFN signaling more directly, we employed RT-PCR to examine IFN transcription level changes both before and after the addition of small molecules during transfection.

Fig. 6 shows the relative quantification of *IFN-β* gene expressions using RT-qPCR. Specifically, the figure shows the ratio of BalanCD cultures with small-molecule additives (IFN inhibitors) to the control cultures over time after transfection. We observed a similar trend among the various inhibitors: The addition of small molecules 4 h before transfection was sufficient to effectively block IFN induction. Furthermore, as time passed, these additives consistently inhibited the expression of *IFN-β*. By the end of the cultivation period, minimal *IFN-β* expression was induced relative to the control condition. In the AMBIC medium, a relatively mild block of IFN signaling was observed for all the inhibitors (see Supplementary Figure 2(b)). Initial supplementation decreased *IFN-β* gene expression by 20–40 %, but no further decrease was observed over time. For both media, these IFN inhibitors successfully limited the induction of IFN, but the degree of IFN signaling pathway inhibition varied. This result is consistent with the productivity

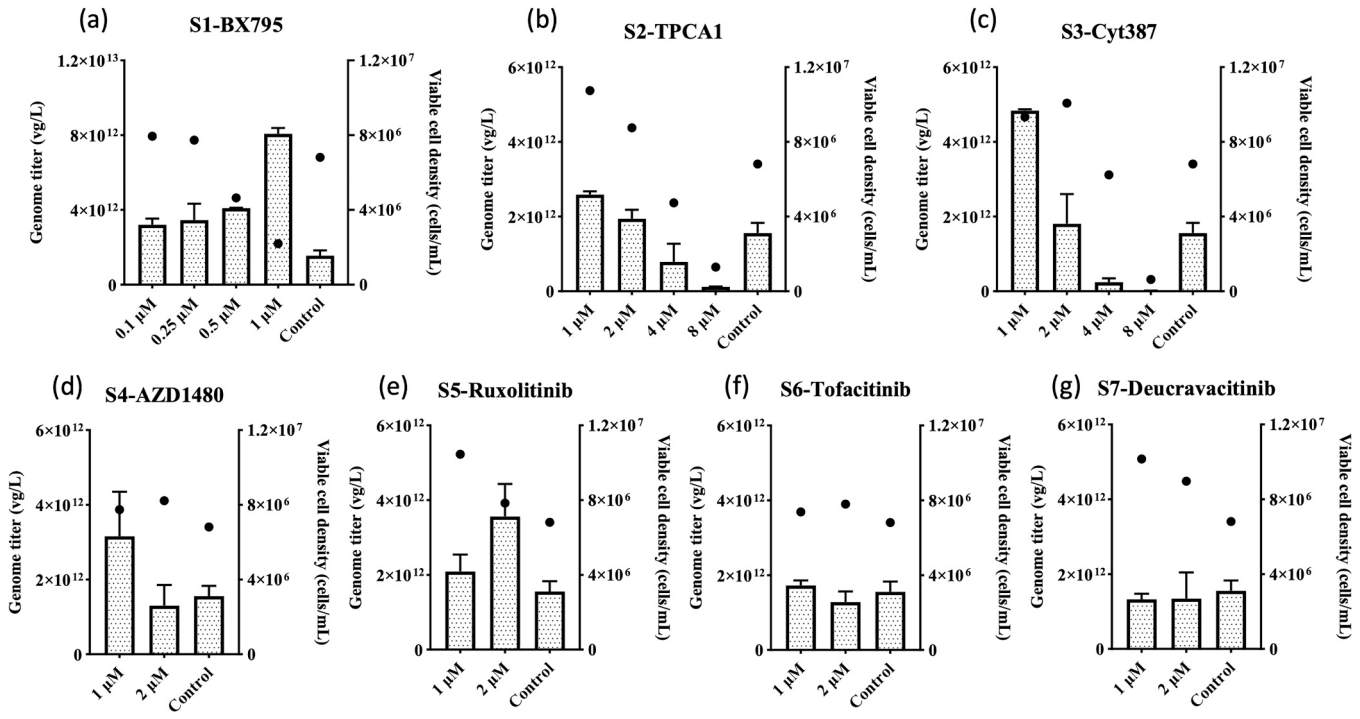

Fig. 3. Screening 2 viable cell density (VCD) and genome titer results in BalanCD medium for S1–S7. Black dots represent the VCD average ($n = 2$) in cells/mL 72 HPT. Refer to Supplementary Table 4 for VCD details for each duplicate. White bars represent the mean and standard deviations of the genome titer in vg/L 72 HPT. The error bar represents the mean and standard deviations for biological duplicates ($n = 2$).

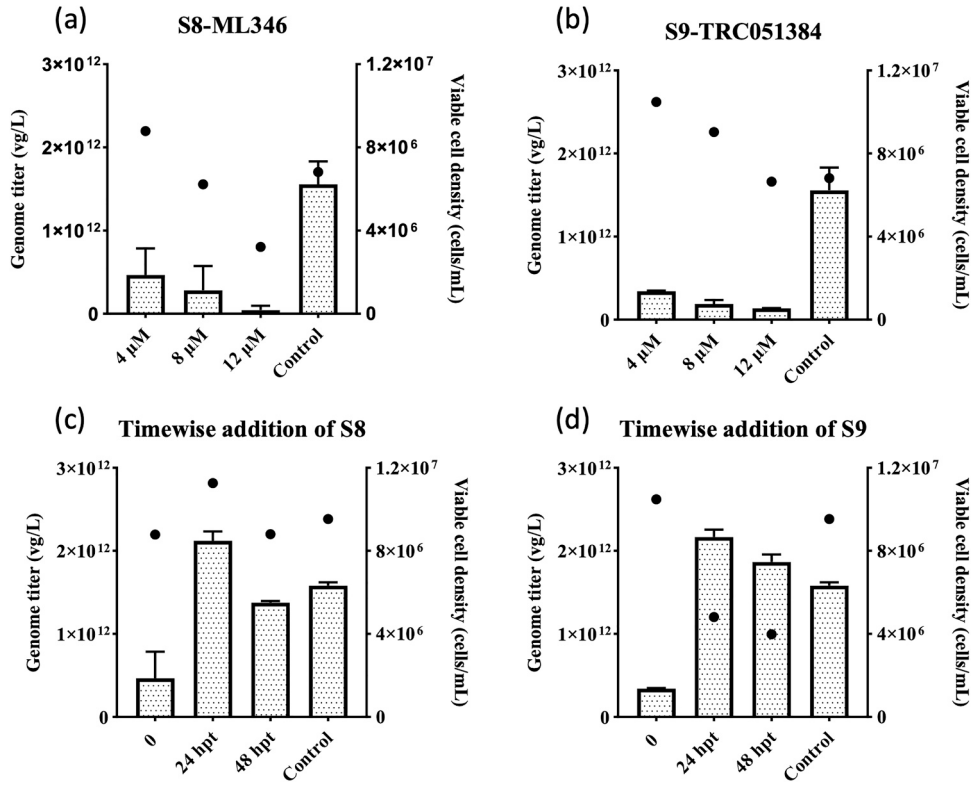

Fig. 4. Evaluation of S8 and S9 on AAV2 production in BalanCD medium. The figure shows various doses and time additions in the deep well. The white bar shows genome titer in vg/L, and the black dots show VCD in cells/mL for S8 (a) and S9 (b), with 4 μM, 8 μM, and 12 μM addition before transfection. The figure shows genome titer in vg/L and VCD in cells/mL for S8 (c) and S9 (d), with 4 μM addition before transfection, 24 HPT, and 48 HPT. The error bar represents the mean and standard deviation of biological duplicates ($n = 2$).

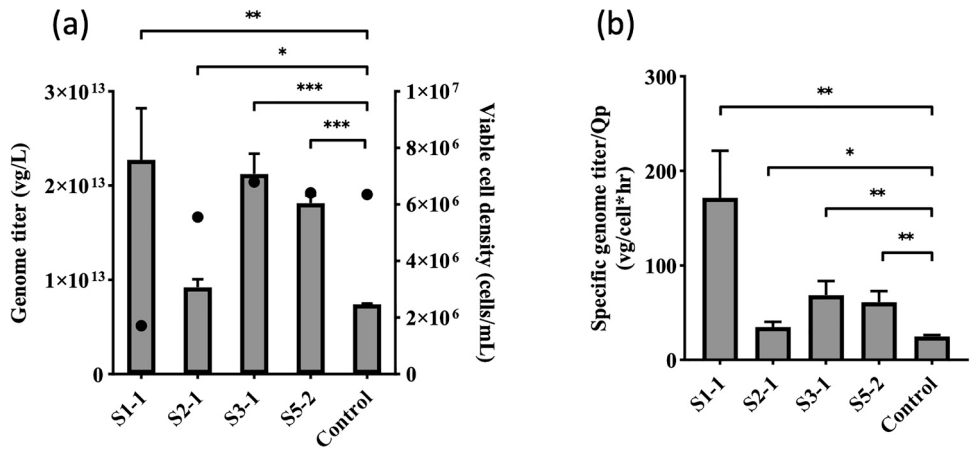

Fig. 5. Confirmation run for AAV production in BalanCD medium on a 125 mL shake flask scale. (a) Genome titer (black bar) in vg/L and VCD (black dots) in cells/mL 72 HPT. The black dots represent the VCD average ($n = 3$) in cells/mL 72 HPT. Refer to Supplementary Table 7 for VCD details for each replicate. (b) Specific productivity Q_p in vg/cell·h 72 HPT. The error bar represents the average and standard deviation for biological triplicates ($n = 3$). The statistical significance of the difference between the treatment and parental groups was evaluated using an unpaired two-tailed student *t*-test. *p* values < .05 were considered statistically significant. *$p < .05$, * *$p < .01$, * **$p < .001$.

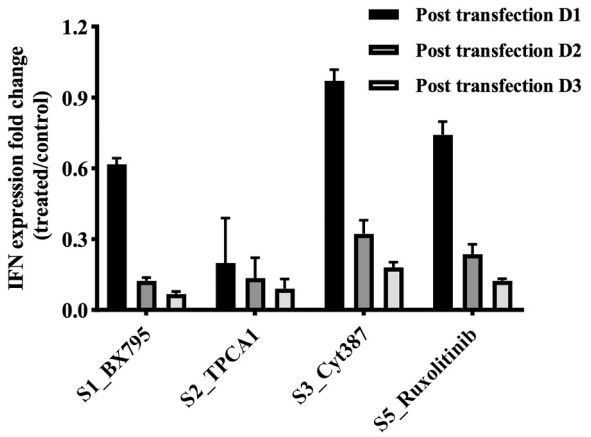

Fig. 6. IFN gene expression fold change (comparing the treated group to the control group) for S1, S2, S3 and S5 over time after transfection. The samples were collected from the shake flask confirmation run in the BalanCD medium. The error bar represents the mean and standard deviations of biological triplicates ($n = 3$).

trend shown in Fig. 5; namely, more obvious and significant titer improvement in the BalanCD medium.

4. Discussion

4.1. Insights from transcriptomic analysis and rationales for supplement candidates

The small molecule additive study was proposed based on the previous transcriptomic investigation of rAAV production (Wang et al., 2023). The significant enrichment of the *Toll-like receptor* (TLR) signaling pathway, the *retinoic acid-inducible gene-I-like receptor* (RLR) signaling pathway, the cytosolic DNA sensing pathway, the downstream Janus kinase-signal transducer as well as the activation of the transcription (JAK–STAT) signaling pathway highlighted the activation of host cell defense mechanism and innate immune responses (Wang et al., 2023) (see Fig. 7).

The host cell's pathogen recognition receptors can detect foreign nucleic acids and viral proteins, which facilitates the recruitment of downstream transcription factors (TBK1, IKK2) and facilitates the phosphorylation of IRF3, IRF7, and NF-kB. These phosphorylated IRFs translocate to the nucleus and trigger the production of IFNs and proinflammatory cytokines (Swiecki and Colonna, 2011). These secreted IFNs can bind to embedded recognition receptors (*IFNAR* with JAK1 and TYK2) in the membrane, thus triggering the dimerization of phosphorylated STAT proteins and the complexation with *IRF9*. This complex translocates to the nucleus and initiates the transcription of ISGs (Raftery and Stevenson, 2017).

Thus, the promising candidates screened in the above-mentioned literature (Stewart et al., 2014) can be used as media supplements to block IFN signaling pathways (see Fig. 7), and restrict IFN production. As a result, to modulate the innate immune response, we supplemented inhibitors of essential IFN signaling proteins (TBK1, IKK2, JAK1, and TYK2) before transfection. In addition, genes related to ER stress and the unfolded protein response (e.g., *HSP70* and *GADD34*) were highly enriched in rAAV production compared to the control condition (Wang et al., 2023). *HSP70* activators were selected as chemical chaperone additives to relieve cell stress during viral protein synthesis and rAAV production. This study explores their impact on post-transfection cell growth and rAAV productivity.

4.2. Impact of supplements on post-transfection cell growth performance and rAAV productivity

Compared to the control (with no additives), small molecule additives generally lowered viable cell density after transfection, thus indicating the suppression of cell growth. A significant improvement in productivity (up to 2-fold) was observed in the BalanCD cultures by supplementing IFN inhibitors before transfection (see Fig. 5(a)), and a productivity increase of approximately 70–80 % was observed in the AMBIC cultures (see Supplementary Figure 2(a)). Suppressed cell growth and improved specific productivity illustrate the tradeoff between overall cell growth performance and specific productivity, and this indicates that more cell resources are directed toward viral production instead of cell growth. The following subsections briefly discuss the mechanisms of these selected small-molecule additives; in particular, how they target IFN signaling pathways and how they affect post-transfection cell growth and rAAV productivity.

4.2.1. TBK inhibitor (S1)

BX795 demonstrates potent and selective inhibition against three key kinases: 3-phosphoinositide-dependent kinase 1 (PDK1), TANK–binding kinase 1 (TBK1), and IκB kinase (IKKε) (Yu et al., 2015).

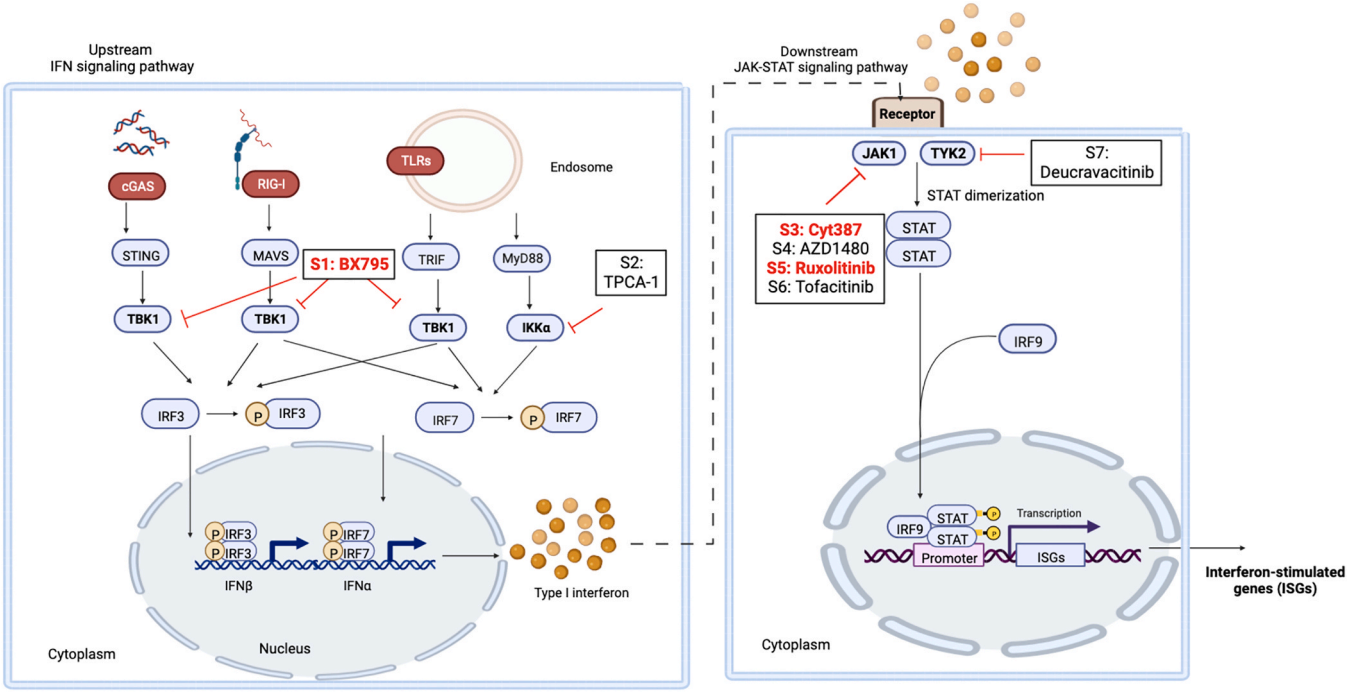

Fig. 7. Innate immune response pathways during rAAV production, including the TLR signaling pathway (initiated in TLRs), the RLR signaling pathway (initiated in RIG-I), the cytosolic DNA sensing pathways (initiated in cGAS), and the downstream JAK–STAT signaling pathways. Supplements are shown as inhibitors to essential signaling proteins during IFN production and ISG transcription. Supplements shown in bold red text significantly improved the rAAV genome titer. The figure was created using BioRender.

Throughout the innate immune signaling cascade transduction, TBK1 serves as a pivotal component that integrates signals from receptors involved in pathogen detection while also modulating the response of IFNs (Stewart et al., 2014). In our study, the BX795 treatment group showed a 1-fold increase in genome titer and exhibited a remarkable 6.5-fold increase in rAAV–specific productivity compared to the control condition in the BalanCD medium. This finding is a strong cross-validation of the previous transcriptomics results, and it suggests that the TBK1–involved pathway may play a prominent role in the innate immune response pathway for rAAV production.

4.2.2. *IKK inhibitor (S2)*

The IKK complex also plays a crucial role in regulating the NF-κB pathway (Podolin et al., 2005), modulating IFN–induced gene expression, and regulating antiviral activity (Du et al., 2012). TPCA-1 (S2) is a selective inhibitor of IKK-2 (Podolin et al., 2005) and exhibits a 22-fold selectivity over IKK-1. TPCA-1 inhibits the NF-κB pathway, thus largely inhibiting the expression of inflammatory genes and the secretion of pro-inflammatory cytokines (Nan et al., 2014; Podolin et al., 2005). TPCA-1 is also reported to directly inhibit JAK1 kinase activity (Cataldi et al., 2015). Furthermore, it is also an inhibitor of *STAT3* and enhances apoptosis (Nan et al., 2014). The literature has reported the induction of apoptosis by TPCA-1, and this further validates the decrease in viable cell density we observed with higher dosages in the cell cultures (Cataldi et al., 2015). In our study, the rAAV productivity was significantly improved in both the BalanCD and AMBIC media. It is noted that, in the BalanCD medium, the specific productivity showed only a 1.7-fold increase compared to the S1 condition (which showed a 6-fold increase). This observation illustrates the less prominent influence of antiviral factors in the IKK2–involved pathways.

4.2.3. *JAK1 and TYK inhibitors (S3–S7)*

JAK1 inhibitors showed the most promising improvement in rAAV productivity. JAK1 and TYK2 play crucial roles in activating the transcription of ISGs within the JAK–STAT pathway. In this study, we selected several small molecules to inhibit the signaling protein JAK1, including S3 (Cyt387), S4 (AZD1480), S5 (ruxolitinib), and S6 (tofacitinib); all of which have slightly different mechanisms of action. Additionally, we utilized S7 (deucravacitinib) to target TYK2. Although S3–S6 have all been reported to inhibit one or more enzymes in the JAK family (Boor et al., 2017; Elli et al., 2019; Lee et al., 2018; Pardanani et al., 2009; Scuto et al., 2011), only S3 (Cyt387) and S5 (ruxolitinib) showed significant improvements in rAAV productivity, resulting in an approximate 1.5-fold to 2-fold increase in rAAV genome titer and a 2-fold to 3-fold increase in specific productivity in the BalanCD medium. Less prominent improvement was achieved in the AMBIC medium: an approximate 20 % increase in genome titer and a 70 % increase in specific productivity. The improvement in titer achieved by adding JAK1 inhibitors confirmed the significant role of JAK1 in innate immune responses during rAAV production. The variable effects of JAK1 inhibitors on viral production may be attributed to their specific inhibition mechanisms. Further experiments are required to confirm and substantiate this hypothesis and speculation. Our results also suggest that TYK2 may not be the dominant gene involved in the innate immune response pathways triggered by rAAV production.

4.2.4. *ER stress relievers (S8–S9)*

HSP70 activators aim to activate the transcription of chemical chaperones and to relieve cell stress caused by the accumulation of viral proteins (Zhang and Wang, 2012). During production of viral vectors, the synthesis of viral proteins leads to many unfolded or misfolded proteins (Kim et al., 2008). The accumulation of these improperly folded proteins, along with ER stress, triggers the host cellular stress response and the unfolded protein response (UPR). Consequently, the UPR attenuates protein synthesis, degrades unfolded or misfolded proteins, and degrades both viral and cellular mRNA through mechanisms such as ER-associated degradation and autophagy–lysosome degradation (Hetz, 2012). The transcription of ER chaperones facilitates recovery from protein translation attenuation. These chaperones help slow translation rates, which improves protein folding and alleviates cellular stress.

This study explored the optimal dosages and addition times designated for these chemical chaperones. S8 resulted in improved rAAV productivity (up to 20 %) when added 24 h post transfection. However, the impact of modulating cellular stress is not as significant as that of regulating the innate immune response. Although host cellular stress response was shown to be enriched in the viral production cultures, the initiated expression of host cell chaperones might be sufficient to overcome the stress induced by the accumulation of unfolded or misfolded proteins. Therefore, the stress induced by rAAV production might not be severe enough to require extra relief from chemical chaperones. Also, the overall rAAV yield in our study, which was lower than the $> 1 \times 10^{14}$ vg/L previously reported (Zhao et al., 2020), could contribute to the relatively low level of cell stress triggered and could limit the productivity impact of supplemented chaperones.

4.3. Distinct behaviors of small molecule additives in various media

It was observed that small molecule additives exhibit distinct behaviors in different culture media, and they affect vector productivity to different extents. A fresh cell culture medium consists of amino acids, trace metals, sugars, growth factors, vitamins, and all other essential components that affect cell growth, transfection efficiency, viral vector titer, and packaging efficiency. Different media contain different levels of these essential components, which alters host cell metabolism as well as the accumulation of metabolites, byproducts, and intermediates. It has been reported that host cell metabolism is reprogrammed during viral infection and production (Prusinkiewicz and Mymryk, 2019; Thaker et al., 2019). The various reprogrammed metabolic pathways initiated by small molecule additives may explain why these IFN inhibitors behave differently in different cell culture media. One literature review discusses the crosstalk between cellular metabolism and innate responses (Zhang et al., 2018). Developing a more mechanistic understanding of titer improvement achieved through small molecules will help further elucidate the observation in this study.

4.4. Applicability and future directions

We demonstrate that the use of small molecules (e.g., IFN inhibitors) can significantly improve rAAV production. We also show that deep well screening can be used to evaluate the optimal dose for each additive in mammalian cell cultures, and the productivity improvement achieved at a small scale can be reproduced in the 30 mL shake flask scale. These IFN inhibitors behave differently in different cell culture media, but they generally exhibit an increase in titer across two different media, indicating general applicability in rAAV manufacturing. It would be worthwhile to validate scalability in a well-controlled bioreactor. There are potential challenges and considerations for scaling up to industrial volumes. A recent study by Wang et al. comparing rAAV production in 50 L stirred tank reactors (STRs) with shake flasks using triple plasmid transfection in HEK293 cells reported some productivity loss. This was attributed to the lower efficiency of transfection mixes prepared in WAVE bags for STRs compared to those vortexed in centrifuge tubes for shake flasks (Wang et al., 2018). Additionally, variability in raw materials used during transient transfection may further affect productivity and product quality at larger scales (Schwartz et al., 2020). Other factors could impact the behaviors of small-molecule additives in the cell cultures, such as the process parameters, the culture medium, and the harvest time (Durocher et al., 2007; Fu et al., 2023; Grieger et al., 2016; Zhao et al., 2020). We also recommend that a set of experiments (using DOE) be conducted using varied process parameters, culture media, and titer levels to fully explore the effects of these small molecule additives on cell cultures and vector production. It would also be intriguing to examine the effects of these small molecules on productivity across different serotypes and transgenes.

Cell line engineering could be further explored as a direction for future research. The knockout of ISG restriction factors (e.g., OAS1, PKR) lead to a 7-fold increase in vector titer during lentiviral vector production in HEK293T cells (Han et al., 2021). The significant enrichment of the antiviral signaling pathway in rAAV production suggests that negative control of the IFN signaling pathway can lower the expression of restriction factors, thus contributing to the enhanced viral production and manufacturing capability of the host cells. Gene silencing or knockout methods could be attempted to restrict the production of IFNs and the expression of ISGs so that host cells can escape the immune response and become more conducive to viral vector production. In addition, the overexpression of ER protein processing genes (e.g., *HSPA5*, *XBP1*, *BCl2*) resulted in a 97 % titer improvement for γ-RV production in HEK293 cells (Formas-Oliveira et al., 2020). Similar strategy has also been conducted and evaluated during rAAV production, resulting in up to 100 % increase in specific productivity (Fu et al., 2024).

This study demonstrates that small molecules can be utilized as additives to optimize medium formulation and improve rAAV production. The addition of small molecules that target innate immune response pathways (e.g., BX795 (a TBK inhibitor), TPCA-1 (an IKK2 inhibitor), Cyt387 (a JAK1 inhibitor), and ruxolitinib (a JAK1 inhibitor)) reduces IFN production and increases rAAV productivity (with up to a 2-fold increase) and increases specific productivity (up to 6-fold). The scalability of this productivity improvement has been demonstrated (from 3 mL in a deep well plate scale to a 30 mL shake flask) as well as its applicability across different media.

Author Contribution Statement

YW, QF, SS, and SY conceived the manuscript. YW and QF conducted data acquisition. YW and QF performed data analysis and interpretation. YW and QF wrote the manuscript. YW, QF, SS and SY edited the manuscript. All authors read and approved the final manuscript.

CRediT authorship contribution statement

Qiang Fu: Writing – review & editing, Writing – original draft, Visualization, Methodology, Investigation, Formal analysis, Data curation. **Yongdan Wang:** Writing – review & editing, Writing – original draft, Visualization, Validation, Methodology, Formal analysis, Data curation, Conceptualization. **Seongkyu Yoon:** Writing – review & editing, Supervision, Resources, Project administration, Funding acquisition, Conceptualization. **Sha Sha:** Writing – review & editing, Supervision, Investigation, Funding acquisition, Conceptualization.

Declaration of Competing Interest

The authors have no competing interests to declare that are relevant to the content of this article. This article does not contain any studies with human participants or animals performed by any of the authors.

Acknowledgement

This work was funded and supported by the Advanced Mammalian Biomanufacturing Innovation Center (AMBIC) through the Industry–University Cooperative Research Center Program under the U.S. National Science Foundation (grant number 2100075). We would like to express our gratitude to all AMBIC member companies for their mentorship and financial support. This work was partially funded by the Massachusetts Life Science Center (MLSC).

Appendix A. Supporting information

Supplementary data associated with this article can be found in the online version at doi:10.1016/j.jbiotec.2025.01.009.

Data availability

Data will be made available on request.

References

Allen, M.J., Boyce, J.P., Trentalange, M.T., Treiber, D.L., Rasmussen, B., Tillotson, B., Reddy, P., 2008. Identification of novel small molecule enhancers of protein production by cultured mammalian cells. Biotechnol. Bioeng. 100 (6), 1193–1204.

Boor, P.P., De Ruiter, P.E., Asmawidjaja, P.S., Lubberts, E., van der Laan, L.J., Kwekkeboom, J., 2017. JAK-inhibitor tofacitinib suppresses interferon alfa production by plasmacytoid dendritic cells and inhibits arthrogenic and antiviral effects of interferon alfa. Transl. Res. 188, 67–79.

Calamini, B., Silva, M.C., Madoux, F., Hutt, D.M., Khanna, S., Chalfant, M.A., Ferguson, J., 2013. ML346: a novel modulator of proteostasis for protein conformational diseases. Probe Rep. NIH Mol. Libr. Program [Internet].

Cataldi, M., Shah, N.R., Felt, S.A., Grdzelishvili, V.Z., 2015. Breaking resistance of pancreatic cancer cells to an attenuated vesicular stomatitis virus through a novel activity of IKK inhibitor TPCA-1. Virology 485, 340–354.

Chang, J., Chen, X., Wang, R., Shi, R., Wang, X., Lu, W., Xia, Q., 2020. High-throughput screening identifies two novel small molecule enhancers of recombinant protein expression. Molecules 25 (2), 353.

Chung, C.-H., Murphy, C.M., Wingate, V.P., Pavlicek, J.W., Nakashima, R., Wei, W., Barton, E., 2023. Production of rAAV By Plasmid Transfection Induces Antiviral and Inflammatory Responses in Suspension HEK293 Cells. Mol. Ther. -Methods Clin. Dev.

Drappier, M., Michiels, T., 2015. Inhibition of the OAS/RNase L pathway by viruses. Curr. Opin. Virol. 15, 19–26.

Du, Z., Whitt, M.A., Baumann, J., Garner, J.M., Morton, C.L., Davidoff, A.M., Pfeffer, L. M., 2012. Inhibition of type I interferon-mediated antiviral action in human glioma cells by the IKK inhibitors BMS-345541 and TPCA-1. J. Interferon Cytokine Res. 32 (8), 368–377.

Duetz, W.A., Ruedi, L., Hermann, R., O'Connor, K., Buchs, J., Witholt, B., 2000. Methods for intense aeration, growth, storage, and replication of bacterial strains in microtiter plates. Appl. Environ. Microbiol. 66 (6), 2641–2646.

Dumbrepatil, A.B., Ghosh, S., Zegalia, K.A., Malec, P.A., Hoff, J.D., Kennedy, R.T., Marsh, E.N.G., 2019. Viperin interacts with the kinase IRAK1 and the E3 ubiquitin ligase TRAF6, coupling innate immune signaling to antiviral ribonucleotide synthesis. J. Biol. Chem. 294 (17), 6888–6898.

Durocher, Y., Pham, P.L., St-Laurent, G., Jacob, D., Cass, B., Chahal, P., Kamen, A., 2007. Scalable serum-free production of recombinant adeno-associated virus type 2 by transfection of 293 suspension cells. J. Virol. Methods 144 (1-2), 32–40.

Ebrahimi, K.H., Howie, D., Rowbotham, J.S., McCullagh, J., Armstrong, F.A., James, W. S., 2020. Viperin, through its radical-SAM activity, depletes cellular nucleotide pools and interferes with mitochondrial metabolism to inhibit viral replication. FEBS Lett. 594 (10), 1624–1630.

Elli, E.M., Baratè, C., Mendicino, F., Palandri, F., Palumbo, G.A., 2019. Mechanisms underlying the anti-inflammatory and immunosuppressive activity of ruxolitinib. Front. Oncol. 9, 1186.

Formas-Oliveira, A.S., Basílio, J.S., Rodrigues, A.F., Coroadinha, A.S., 2020. Overexpression of ER protein processing and apoptosis regulator genes in human embryonic kidney 293 cells improves gene therapy vectors production. Biotechnol. J. 15 (9), 1900562.

Fu, Q., Lee, Y.S., Green, E.A., Wang, Y., Park, S.Y., Polanco, A., Yoon, S., 2023. Design space determination to optimize DNA complexation and full capsid formation in transient rAAV manufacturing. Biotechnol. Bioeng.

Fu, Q., Polanco, A., Lee, Y.S., Yoon, S., 2023. Critical challenges and advances in recombinant adeno-associated virus (rAAV) biomanufacturing. Biotechnol. Bioeng.

Fu, Q., Wang, Y., Qin, J., Xie, D., McNally, D., Yoon, S., 2024. Enhanced ER protein processing gene expression increases rAAV yield and full capsid ratio in HEK293 cells. Appl. Microbiol. Biotechnol. 108 (1), 459.

Grieger, J.C., Soltys, S.M., Samulski, R.J., 2016. Production of recombinant adeno-associated virus vectors using suspension HEK293 cells and continuous harvest of vector from the culture media for GMP FIX and FLT1 clinical vector. Mol. Ther. 24 (2), 287–297.

Han, J., Tam, K., Tam, C., Hollis, R.P., Kohn, D.B., 2021. Improved lentiviral vector titers from a multi-gene knockout packaging line. Mol. Ther. -Oncolytics 23, 582–592.

Hetz, C., 2012. The unfolded protein response: controlling cell fate decisions under ER stress and beyond. Nat. Rev. Mol. Cell Biol. 13 (2), 89–102.

Honarmand Ebrahimi, K., Vowles, J., Browne, C., McCullagh, J., James, W.S., 2020. ddhCTP produced by the radical-SAM activity of RSAD2 (viperin) inhibits the NAD + -dependent activity of enzymes to modulate metabolism. FEBS Lett. 594 (10), 1631–1644.

Hwang, S.J., Jeon, C.J., Cho, S.M., Lee, G.M., & Yoon, S.K.J.B. p. (2011). Effect of chemical chaperone addition on production and aggregation of recombinant flag-tagged COMP-angiopoietin 1 in chinese hamster ovary cells. *27*(2), 587-591.

Kim, I., Xu, W., Reed, J.C., 2008. Cell death and endoplasmic reticulum stress: disease relevance and therapeutic opportunities. Nat. Rev. Drug Discov. 7 (12), 1013–1030.

Lee, S., Shah, T., Yin, C., Hochberg, J., Ayello, J., Morris, E., Cairo, M.S., 2018. Ruxolitinib significantly enhances in vitro apoptosis in Hodgkin lymphoma and primary mediastinal B-cell lymphoma and survival in a lymphoma xenograft murine model. Oncotarget 9 (11), 9776.

Lu, M., Lee, Z., Hu, W.S., 2024. Multi-omics kinetic analysis of recombinant adeno-associated virus production by plasmid transfection of HEK293 cells. Biotechnol. Prog., e3428

Meyer, H.J., Turincio, R., Ng, S., Li, J., Wilson, B., Chan, P., Wong, A.W., 2017. High throughput screening identifies novel, cell cycle-arresting small molecule enhancers of transient protein expression. Biotechnol. Prog. 33 (6), 1579–1588.

Mohanan, A., Deshpande, S., Jamadarkhana, P.G., Kumar, P., Gupta, R.C., Chauthaiwale, V., Dutt, C., 2011. Delayed intervention in experimental stroke with TRC051384–a small molecule HSP70 inducer. Neuropharmacology 60 (6), 991–999.

Nan, J., Du, Y., Chen, X., Bai, Q., Wang, Y., Zhang, X., Wang, Q., 2014. TPCA-1 is a direct dual inhibitor of STAT3 and NF-κB and regresses mutant EGFR-associated human non–small cell lung cancers. Mol. Cancer Ther. 13 (3), 617–629.

Onitsuka, M., Tatsuzawa, M., Asano, R., Kumagai, I., Shirai, A., Maseda, H., 2014. Trehalose suppresses antibody aggregation during the culture of Chinese hamster ovary cells. bioengineering 117 (5), 632–638.

Pardanani, A., Lasho, T., Smith, G., Burns, C., Fantino, E., Tefferi, A., 2009. CYT387, a selective JAK1/JAK2 inhibitor: in vitro assessment of kinase selectivity and preclinical studies using cell lines and primary cells from polycythemia vera patients. Leukemia 23 (8), 1441–1445.

Podolin, P.L., Callahan, J.F., Bolognese, B.J., Li, Y.H., Carlson, K., Davis, T.G., Roshak, A. K., 2005. Attenuation of murine collagen-induced arthritis by a novel, potent, selective small molecule inhibitor of IκB kinase 2, TPCA-1 (2-[(aminocarbonyl) amino]-5-(4-fluorophenyl)-3-thiophenecarboxamide), occurs via reduction of proinflammatory cytokines and antigen-induced T cell proliferation. J. Pharmacol. Exp. Ther. 312 (1), 373–381.

Prusinkiewicz, M.A., Mymryk, J.S., 2019. Metabolic reprogramming of the host cell by human adenovirus infection. Viruses 11 (2), 141.

Raftery, N., Stevenson, N.J., 2017. Advances in anti-viral immune defence: revealing the importance of the IFN JAK/STAT pathway. Cell. Mol. Life Sci. 74, 2525–2535.

Scarrott, J.M., Johari, Y.B., Pohle, T.H., Liu, P., Mayer, A., James, D.C., 2023. Increased recombinant adeno-associated virus production by HEK293 cells using small molecule chemical additives. Biotechnol. J. 18 (3), 2200450.

Schwartz, M.D., Emerson, S.G., Punt, J., Goff, W.D., 2020. Decreased naïve T-cell production leading to cytokine storm as cause of increased COVID-19 severity with comorbidities. Aging Dis. 11 (4), 742.

Scuto, A., Krejci, P., Popplewell, L., Wu, J., Wang, Y., Kujawski, M., Kretzner, L., 2011. The novel JAK inhibitor AZD1480 blocks STAT3 and FGFR3 signaling, resulting in suppression of human myeloma cell growth and survival. Leukemia 25 (3), 538–550.

Stewart, C.E., Randall, R.E., Adamson, C.S., 2014. Inhibitors of the interferon response enhance virus replication in vitro. PLoS One 9 (11), e112014.

Strasser, L., Boi, S., Guapo, F., Donohue, N., Barron, N., Rainbow-Fletcher, A., Bones, J., 2021. Proteomic Landscape of Adeno-Associated Virus (AAV)-Producing HEK293 Cells. Int. J. Mol. Sci. 22 (21), 11499.

Swiecki, M., Colonna, M., 2011. Type I interferons: diversity of sources, production pathways and effects on immune responses. Curr. Opin. Virol. 1 (6), 463–475.

Thaker, S.K., Ch'ng, J., Christofk, H.R., 2019. Viral hijacking of cellular metabolism. BMC Biol. 17, 1–15.

Wang, P., Bhat, V., Dong, W., Pham, H., Pubill, S., Kasaraneni, N., Seth, A., 2018. Establishment of a scalable manufacturing platform for in-silico-derived ancestral adeno-associated virus vectors. Cell Gene Ther. Insights.

Wang, Y., Fu, Q., Lee, Y.S., Sha, S., Yoon, S., 2023. Transcriptomic features reveal molecular signatures associated with recombinant adeno-associated virus production in HEK293 cells. Biotechnol. Prog., e3346

Wang, Y., Fu, Q., Park, S.Y., Lee, Y.S., Park, S.-Y., Lee, D.-Y., Yoon, S., 2024. Decoding cellular mechanism of recombinant adeno-associated virus (rAAV) and engineering host-cell factories toward intensified viral vector manufacturing. Biotechnol. Adv., 108322

Warga, E., Anderson, J., Tucker, M., Harris, E., Elmer, J., 2023. Transcriptomic analysis of the innate immune response to in vitro transfection of plasmid DNA. Mol. Ther. -Nucleic Acids 31, 43–56.

Yang, W.C., Lu, J., Nguyen, N.B., Zhang, A., Healy, N.V., Kshirsagar, R., Huang, Y.-M., 2014. Addition of valproic acid to CHO cell fed-batch cultures improves monoclonal antibody titers. Mol. Biotechnol. 56, 421–428.

Yu, T., Yang, Y., Yin, D.Q., Hong, S., Son, Y.-J., Kim, J.-H., Cho, J.Y., 2015. TBK1 inhibitors: a review of patent literature (2011–2014). Expert Opin. Ther. Pat. 25 (12), 1385–1396.

Zhang, S., Carriere, J., Lin, X., Xie, N., Feng, P., 2018. Interplay between cellular metabolism and cytokine responses during viral infection. Viruses 10 (10), 521.

Zhang, L., Wang, A., 2012. Virus-induced ER stress and the unfolded protein response. Front. Plant Sci. 3, 293.

Zhao, H., Lee, K.-J., Daris, M., Lin, Y., Wolfe, T., Sheng, J., Meisen, W.H., 2020. Creation of a high-yield AAV vector production platform in suspension cells using a design-of-experiment approach. Mol. Ther. -Methods Clin. Dev. 18, 312–320.

Zhou, X., Michal, J.J., Zhang, L., Ding, B., Lunney, J.K., Liu, B., Jiang, Z., 2013. Interferon induced IFIT family genes in host antiviral defense. Int. J. Biol. Sci. 9 (2), 200.